processes

MDPI

Article

Enhancing Barite Carbothermal Reduction with Brown Coal by Compaction of the Charge

Tlek Ketegenov [1], Kaster Kamunur [1,2], Aisulu Batkal [1] and Rashid Nadirov [1,2,*]

[1] Institute of Combustion Problems, Almaty 050012, Kazakhstan
[2] Department of General and Inorganic Chemistry, Al-Farabi Kazakh National University, Almaty 050040, Kazakhstan
* Correspondence: nadirov.rashid@gmail.com; Tel.: +7-747-452-05-25

Abstract: Barium sulfide is an important intermediate in the manufacture of ceramics, glass, plastics, and pharmaceutical products. This substance is traditionally obtained by carbothermal reduction of barite (barium sulfate) in the presence of a carbon-containing reducing agent, mainly coal. Herein, it is demonstrated that compaction of the charge before the carbothermal reduction significantly enhances the conversion of barium sulfate to sulfide due to an increase in the contact time of carbon monoxide with barite in a compact sample in comparison with a powder sample. In the presence of NaOH as a catalyst, the degree of conversion of barium sulfate in a compact sample was 0.95–0.97 upon roasting at 1150 °C for 65 min, while in a powder sample this value did not exceed 0.6. Furthermore, charge compaction reduced the conversion activation energy (136 vs. 264 kJ mol^{-1}), which could be a tool for reducing the energy intensity of obtaining barium sulfide from its sulfate.

Keywords: barite; carbothermal reduction; compaction; barium sulfide

Citation: Ketegenov, T.; Kamunur, K.; Batkal, A.; Nadirov, R. Enhancing Barite Carbothermal Reduction with Brown Coal by Compaction of the Charge. *Processes* **2022**, *10*, 2323. https://doi.org/10.3390/pr10112323

Academic Editor: Adam Smoliński

Received: 19 September 2022
Accepted: 4 November 2022
Published: 8 November 2022

1. Introduction

Barium sulfide (BaS) is an important chemical material and is used as an intermediate product in the industrial processes of obtaining barium compounds, widely applied in ceramics, glass, plastic, and pharmaceutical industries [1–4]. The traditional way to obtain barium sulfide involves carbothermal reduction of barite (barium sulfate, $BaSO_4$). Barite ore or concentrate is reduced by carbon-containing reductants, predominantly by coal or coke, in a rotatory kiln or fluidized bed reactor according to the above reactions [5–9].

It has been proven in numerous papers from the early 1950s [10] that the solid-state contact point between barite and carbon-containing reductant (Equation (1)) is the initial stage of the reduction process. It has been found that the rate of the reaction between $BaSO_4$ and CO (Equation (2)) is considerably higher than that of Equation (3) [8,11]. Thus, the overall rate of carbothermal reduction is controlled by the so-called Boudouard reaction, representing the interaction of solid carbon with carbon dioxide to form carbon monoxide (Equation (3)) [8,12]. The formation of CO enhances the barite reduction rate, meaning that an increase in the gasification rate has a beneficial effect on the entire process.

$$BaSO_4 + 4C = BaS + 4CO \quad (1)$$

$$BaSO_4 + 4CO = BaS + 4CO_2 \quad (2)$$

$$C + CO_2 = 2CO \quad (3)$$

The rate of the gasification reaction (3) can be significantly enhanced by using catalysts, which include alkaline additives such as caustic soda or salts of alkali metals [10,13,14]. The presence of a catalyst results in a decrease in activation energy accompanied by a corresponding increase in the pre-exponential factor. Jagtap et al. [12] demonstrated that the reaction rate constant for the reduction of barite with carbon was increased by 2.75 times

when 5 wt.% of sodium carbonate was added to the charge. The addition of 7.5 wt.% of this salt decreased the activation energy of the barite carbothermal reduction from 35.3 to 6.8 kcal/mol [15]. Gokarn et al. [16] have shown the positive effect of sodium metavanadate on the barite carbothermal reduction at temperatures lower than 920 °C. The presence of a catalyst ensures a higher number of active sites in the reaction environment, although the mechanism of catalytic action is not completely understood. Electron-transfer and oxygen-transfer theories are recognized as the most likely explanations for the catalytic effect [10]. According to the electron-transfer theory, a transfer of electrons to or from the carbon substrate occurs, resulting in a redistribution of π-electrons in a carbon structure, the weakening of the carbon–carbon bonds at the edges of substrate sheets, and an increase in the strength of carbon–oxygen bonds during oxidation. The oxygen-transfer mechanism supposes that the catalyst acts as an oxygen carrier that promotes the transfer of oxygen from the gas phase to the carbon surface. In any event, the need to use a catalyst in the process of carbothermal reduction of barite is not questioned.

The use of catalysts makes it possible to carry out the carbothermal reduction of barite at lower temperatures than in the absence of catalysts; moreover, an increase in temperature sometimes hampers the carbothermal reduction in the presence of a catalyst [16]. This is due to the so-called compensation effect in the catalytic gasification of carbon [17]. Upon reaching a certain temperature of carbothermal reduction, a decrease in the activation energy in the presence of a catalyst is compensated by an increase in the pre-exponential factor, meaning that the reaction rate constant does not depend on the amount of catalyst.

The carbothermal reduction of barite is a complex process, including solid–solid and gas–solid reactions, heat transfer, and mass transfer, any of which can occur simultaneously. The conversion of $BaSO_4$ to BaS depends on several factors, primarily temperature and thermal processing duration. However, there are less obvious factors as well, such as the state of the charge (compacted or powder). Despite a few papers devoted to barite carbothermal reduction, only one has considered the effect of the compacting method on the process effectiveness; Jamshidi and Salem investigated the role of the extreme fusion process on the kinetic parameters of the process at temperatures of 850, 900, 950, and 1050 °C in air atmosphere and in both the presence and absence of catalysts [18]. This is not enough for a full assessment of the impact of charge shaping on the conversion degree and kinetic parameters of the carbothermal reduction.

On the other hand, interest in carbothermal reduction is currently quite high, with the processing magnesia source [19], low-grade pyrolusite [20], iron source [21], red mud [22], silicon source [23], zinc oxide from battery waste [24], and copper smelter slag [25] all being investigated. Therefore, the issue of charge preparation before reduction is important.

In the present work, we compared two modes of reduction of barite concentrate with brown coal in the presence of sodium hydroxide as a catalyst by varying the state of the charge (compacted sample and powder sample). The process of barium sulfate conversion to barium sulfide was discussed using a modified volume reaction model.

2. Materials and Methods

2.1. Materials

Barite concentrate (89% $BaSO_4$) and brown coal (92% C) were supplied by Vostochnoe Ore Mining LLP, Kazakhstan. The composition of barite concentrate was determined by atomic emission spectroscopy (Optima 8000, Perkin Elmer, Waltham, MA, USA) as follows: wt%: Ba 53.19; S 12.22; Si 4.48; Fe 0.75; Ca 0.25; Al 0.95; Mg 0.20.

Iodine, hydrochloric acid, sodium thiosulfate, and sodium hydroxide were of reagent grade and used without further purification.

2.2. Sample Preparation

Two types of samples were prepared for the experiments.

To obtain the first type, 12.50 g of ground (<100 μm particle sizes) of barite concentrate was thoroughly mixed with 3.50 g of brown coal (<90 μm particle sizes) as well as with

0.50 mL of 10% NaOH solution using a Waring LB20ES laboratory blender. The resulting wet mixture was pressed (150 kg/cm^2) to obtain a cylinder (20 mm in diameter and about 20 mm in height) and the cylinder was dried to constant weight. This type of sample is hereinafter referred to as a compacted barite sample.

To obtain the second type, 12.50 g of ground (<100 μm particle sizes) of barite concentrate was thoroughly mixed with 3.50 g of brown coal (<90 μm particle sizes) as well as with 0.05 g of NaOH using the aforementioned laboratory blender. This type of sample is hereinafter referred to as a powder barite sample.

2.3. Carbothermal Reduction

2.3.1. Compacted Barite Sample

A muffle furnace (SNOL 6.7/1300, Russia) equipped with a type K thermocouple was used for the thermal treatment of the samples. When the required furnace temperature was reached, a silica boat containing the nine samples was placed in the less hot zone of the furnace for 8 min. Then, the sample-containing boat was placed into the central zone of the furnace where the desired temperature was maintained. This moment was counted as zero time. Because the reactor system was not sufficiently airtight, air was assumed to be present in the furnace. Upon reaching the predetermined high-temperature treatment time of the samples, one sample was removed from the boat and was cooled to room temperature before measuring the BaS percentage. After room temperature was reached, the sample was cut into two parts parallel to the base to obtain a cross-section. Then, from the centre of the section, two circles were designated with diameters of 3 and 6 mm, respectively. The material bounded by the inner circumference is hereinafter referred to as zone A, while the material delimited by two circles is designated as zone B; in turn, the material bounded by the outer circumference and the surface of the cylinder is designated as zone C (see Figure 1).

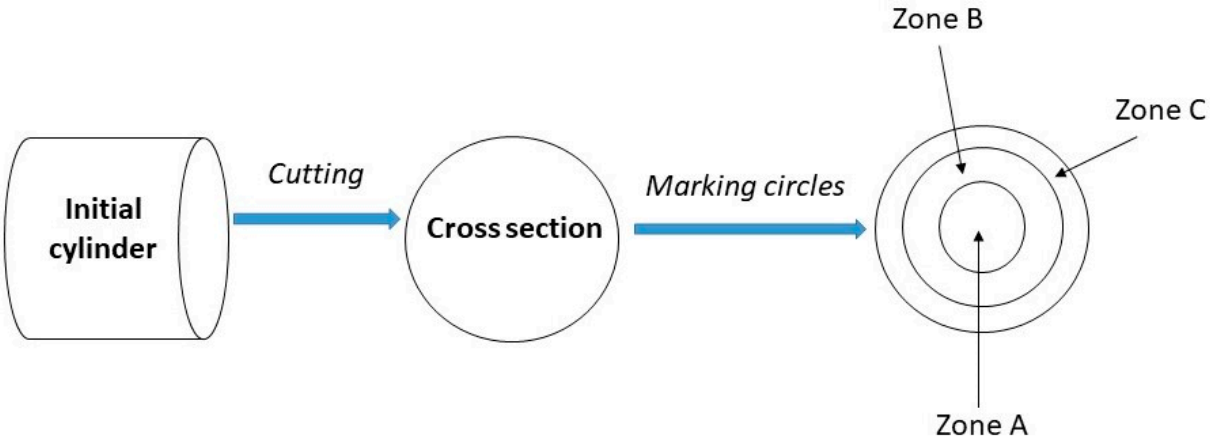

Figure 1. Preparing thermally treated compacted (cylindrical) barite sample for subsequent sampling.

The material from each zone was carefully sampled separately in order to determine the conversion of barium sulfate to barium sulfide.

Images of starting (unheated) and roasted (1150 °C, 65 min) compacted samples are presented in Figure 2.

2.3.2. Powder Barite Sample

In the case of the powder barite sample, the heat treatment procedure was the same as for the compacted barite sample; however, one sample was subjected to heating, and sampling was carried out from the entire volume of the boat.

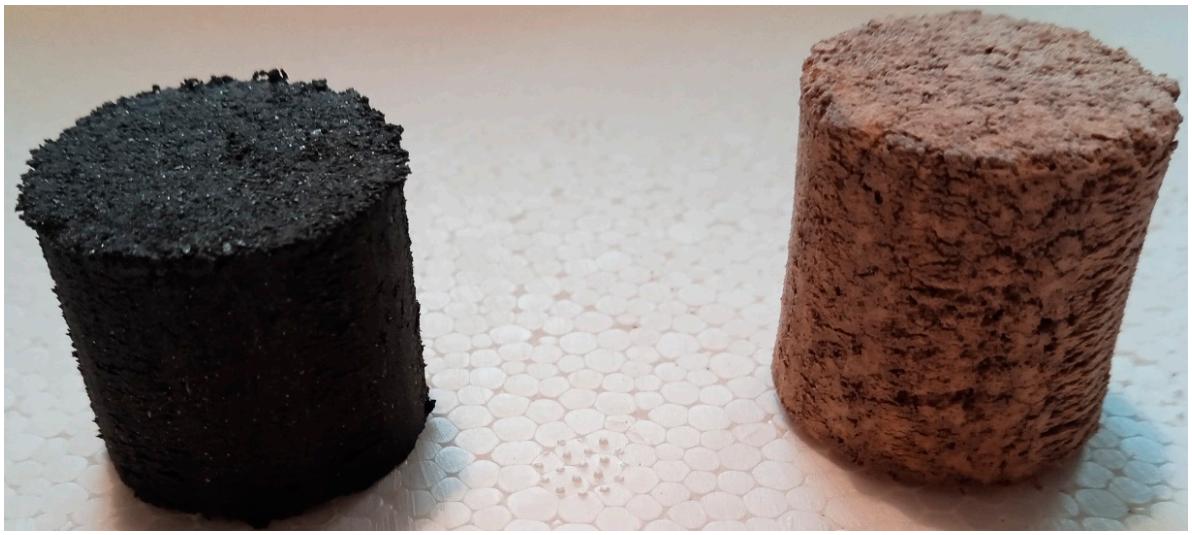

Figure 2. Starting (**left**) and roasted at 1150 °C for 65 min (**right**) compacted samples.

2.4. Characterization

The powder materials were characterized by X-ray diffraction (XRD) in a D8 Advance (Bruker, Billerica, MA, USA) using α-Cu radiation, as well as by scanning electron microscopy (SEM) using a Quanta 200i 3D (FEI, USA).

2.5. Barium Sulfide Percentage Measuring

The iodometry method was applied for measuring the BaS content in the ground product [25]. This method is based on the consumption of elemental iodine for the oxidation of sulfide ions (Equation (4)) and the subsequent determination of residual iodine by titration with sodium thiosulfate (Equation (5)):

$$S^{2-} + I_2 = {SO_4}^{2-} + I^- \quad (4)$$

$$2Na_2S_2O_3 + I_2 = 2NaI + Na_2S_4O_6 \quad (5)$$

Primarily, 50 mL of 0.5 N iodine solution was mixed with 50 mL of 1 N hydrochloric acid solution, then 2 g of the product was added to 100 mL of deionized hot water and stirred for 5–7 min. The suspension was mixed with the solution obtained at the previous stage, and the resulting solution was titrated with 0.1 N sodium thiosulfate in the presence of starch as an indicator to obtain a pale yellow colour. The BaS percentage (*C*) was calculated by Equation (6):

$$C = 8.17 \left(\frac{N_1V_1 - N_2V_2}{W} \right) \quad (6)$$

where N_1V_1 and N_2V_2 are the total moles of iodine and sodium thiosulfate, respectively, and *W* is the weight of the ground sample.

3. Results and Discussion

3.1. Compacted Sample

Particles of barite in a compacted cylindrical sample have different environments. The material in the central zone (zone A, Figure 1) is surrounded by a mixture of barite and coal. The barite in the outer zone (zone C, Figure 1) is surrounded, on the one hand, by a mixture of barite and coal, and on the other borders the atmosphere (in our case, an inert atmosphere of nitrogen). Thus, it seemed informative to compare the results of the carbothermal reduction of barite located in different zones (A, B, C) of the cylinder.

The effect of operating temperature and treatment duration on the conversion of the compacted barite sample to barium sulfide (zone A) is presented in Figure 3.

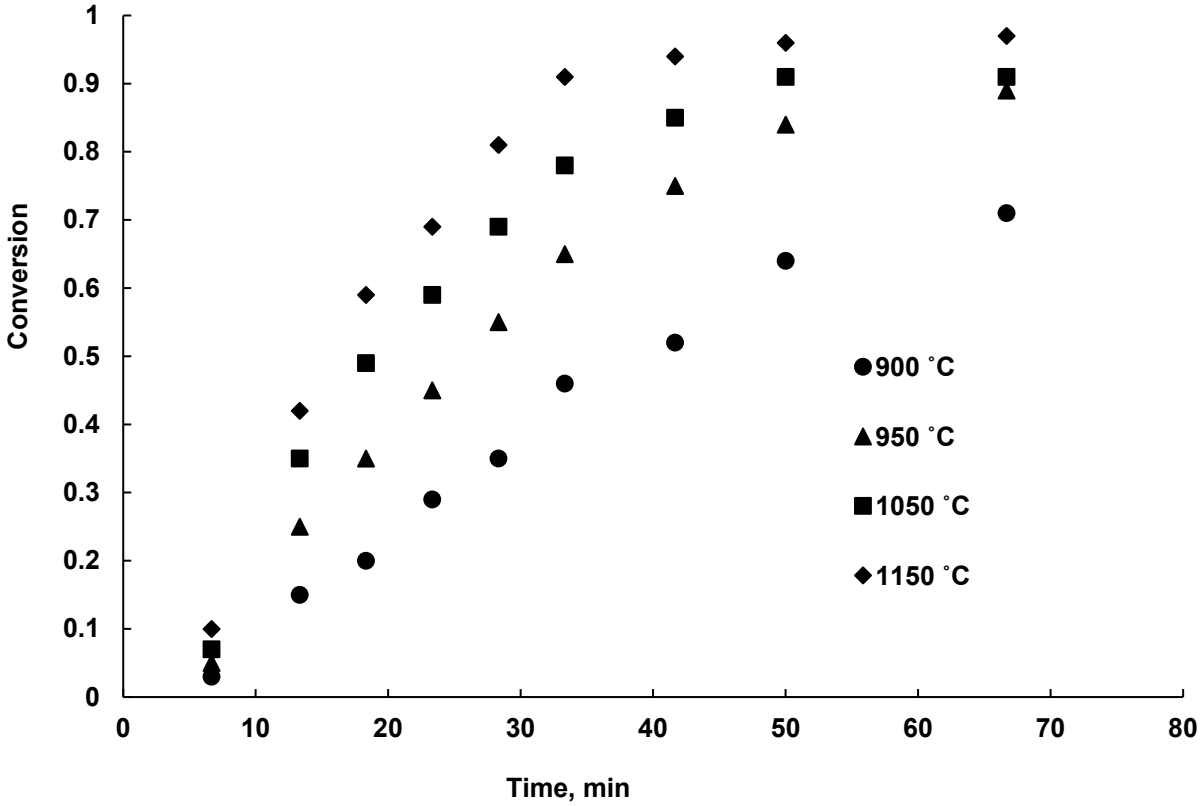

Figure 3. Conversion-time plots for the reduction of barite compacted samples (zone A; see Figure 1) with brown coal.

At all temperatures studied, the conversion degree increased with an increase in the duration of treatment, and eventually reached a plateau. The maximum conversion was 0.97 (97%) at 1150 °C and 65 min. In the first 7 min, a very low conversion was achieved in all cases (0.03, 0.05, 0.07, and 0.11 at 900, 950, 1050, and 1150 °C, respectively). The conversion rate then accelerated, followed by deceleration at the end. The behaviour observed from the conversion-time plots is in good agreement with that described in papers devoted to the carbothermal reduction of barite [12,18].

XRD patterns of unheated and two roasted (1150 °C, 18 min and 1150 °C, 65 min) samples are presented in Figure 4. An increase in the duration of roasting the charge contributed to an increase in the intensity of the peaks corresponding to barium sulfide; these results are in agreement with the data shown in Figure 3.

A modified volume reaction (MVR) model, developed by Kasaoka et al. [26], was applied to the conversion-time plots presented in Figure 3. The model proposed by Kasaoka and Sakata [27] can be presented as the following Equation (7):

$$x = 1 - \exp\left(-a\theta^b\right) \tag{7}$$

where x is the fractional conversion, θ is the thermal treatment duration (in seconds), and a and b are constants.

The model presented in Equation (7) is applicable in all cases of carbothermal reaction, whether a catalyst is used or not [12].

The constant parameter a is related to the kinetic rate constant, and is temperature-sensitive, whereas the constant parameter b is related to the physical changes taking place in the carbon matrix.

The linearized form of Equation (7) can be presented as Equation (8):

$$\ln(-\ln(1-x)] = \ln a + b \ln \theta \tag{8}$$

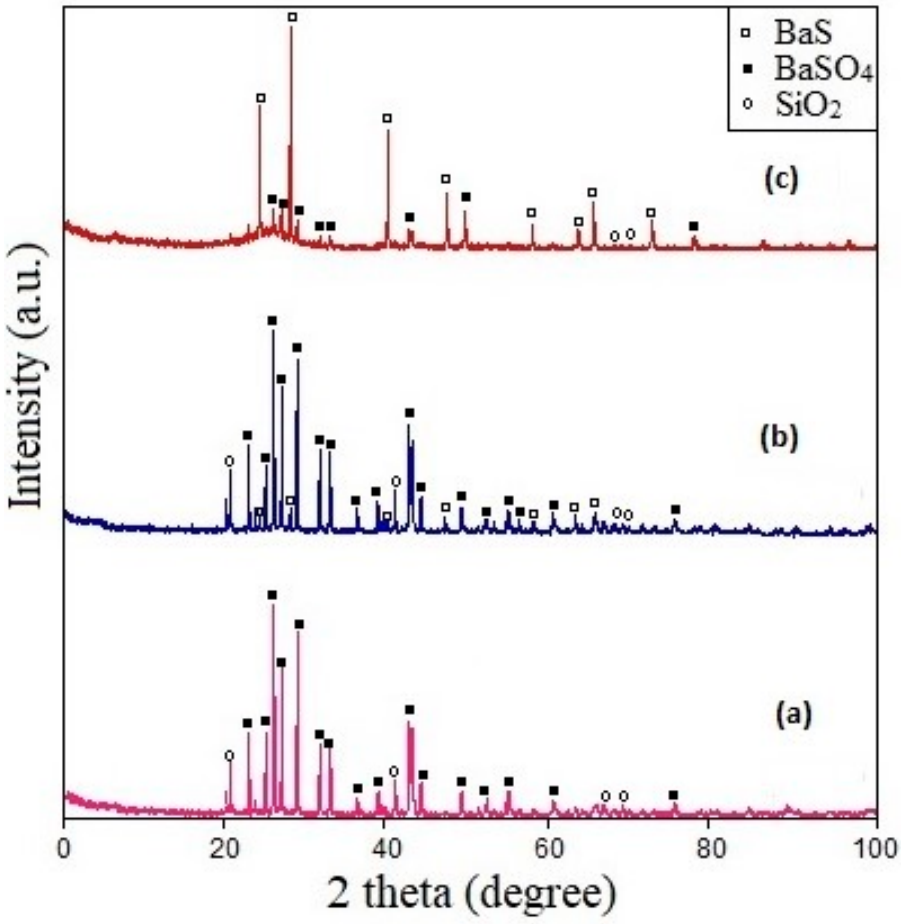

Figure 4. XRD patterns of unheated (**a**) and roasted (1150 °C, 18 min (**b**) and 1150 °C, 65 min (**c**)) samples.

Model parameters a and b can be calculated from the slopes and intercepts; then, by using a and b values, the rate constants are calculated according to the expression suggested by Kasaoka et al. [27]:

$$k(x) = a^{\frac{1}{b}} b[-\ln(1-x)]^{\frac{b-1}{b}} \quad (9)$$

To simplify calculations, the Erofeev equation can be applied to the MVR model:

$$\ln(-\ln(1-x)] = \ln k + n \ln \theta \quad (10)$$

Herein, k is the rate constant, n is the constant related to the reaction mechanism, and x and θ have the same values as in Equations (7)–(9).

The kinetic plots obtained using the data from Figure 3 and the MVR model for the four operating temperatures are shown in Figure 5. The X-axis (argument) shows the values of the logarithm of time (in seconds), while the Y-axis (function) shows the calculated values of ln $(-\ln (1-x)]$).

At all investigated temperatures, the process of the barite compacted sample carbothermal reduction (zone A) with coal fit the MVR model very well due to the good linear tendency of the plots.

We now consider the conversion of barite located in the outer zone (zone C). The influence of operating temperature and treatment duration on the conversion of the compacted barite sample to barium sulfide (zone C) in an oxygen-free environment is presented in Figure 6.

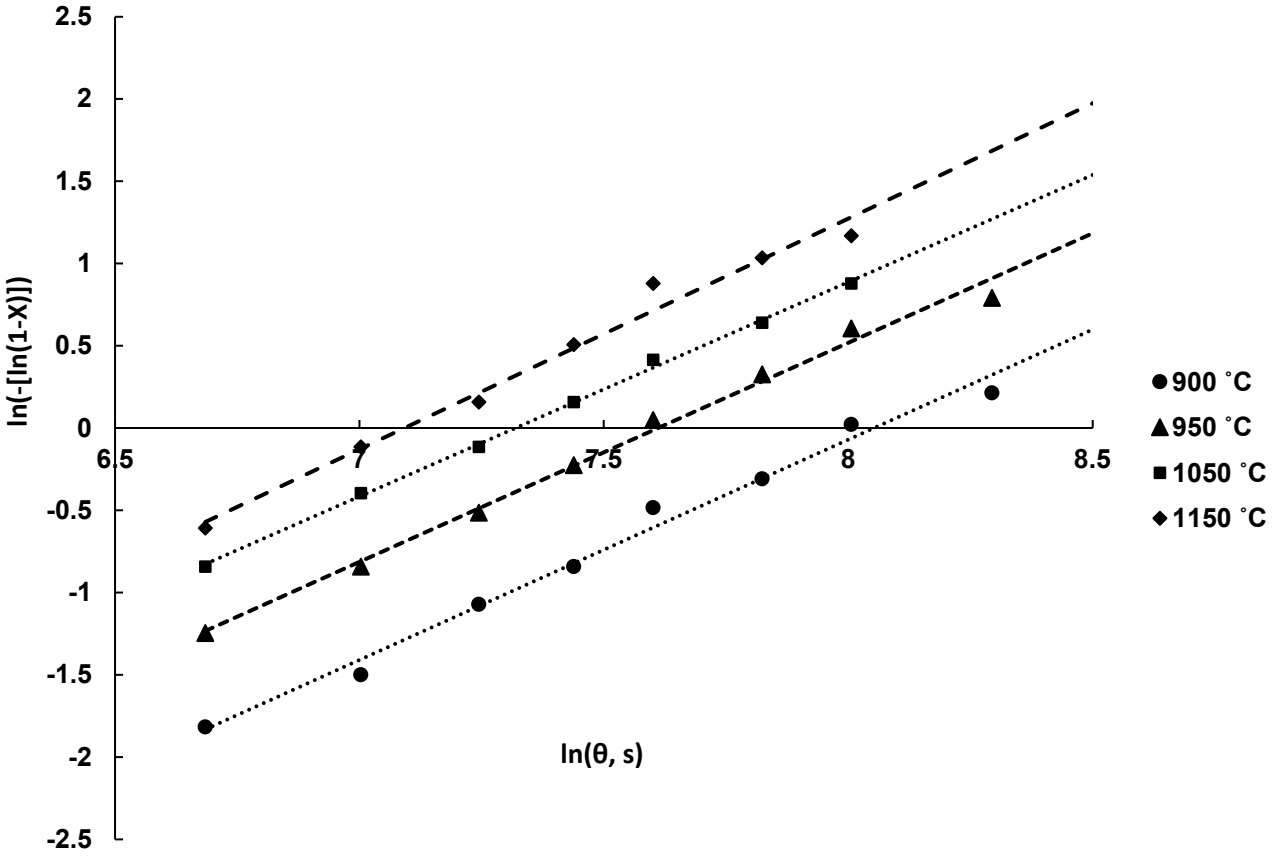

Figure 5. Application of the MVR model to the reduction of barite compacted samples (zone A; see Figure 1) by brown coal in an oxygen-free environment.

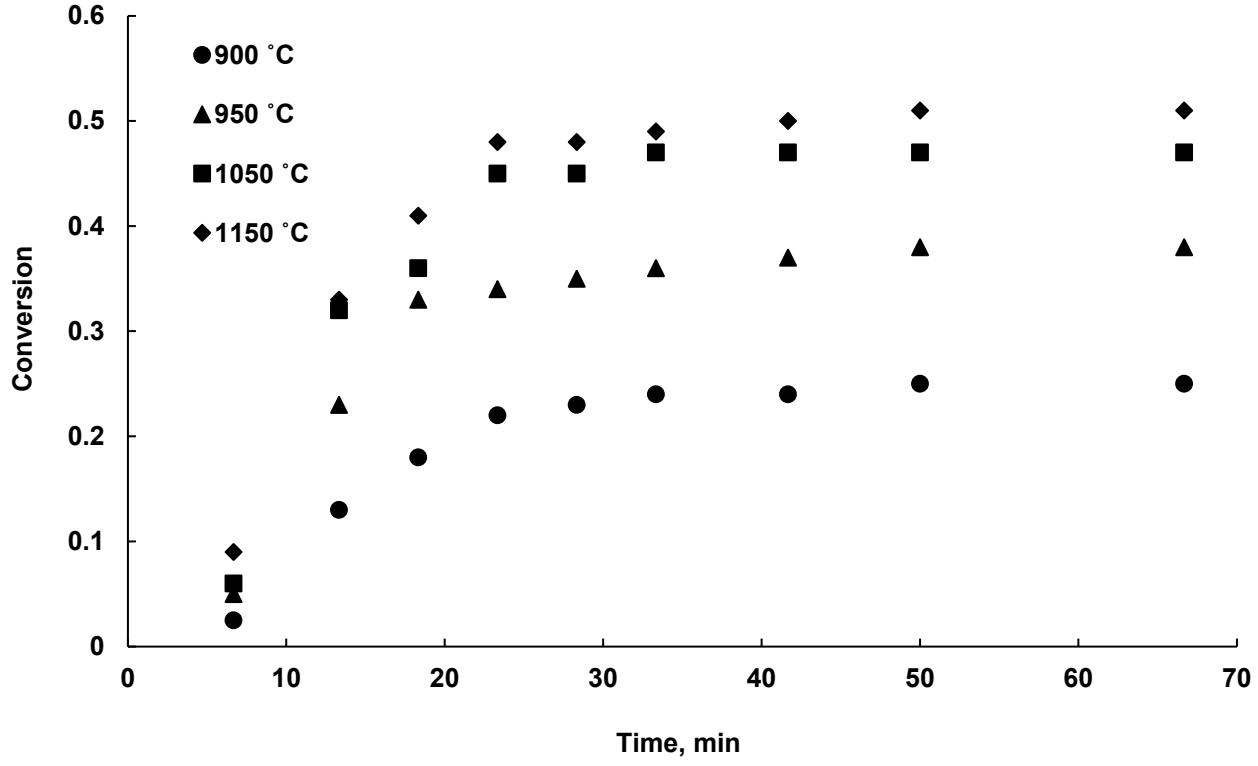

Figure 6. Conversion-time plots for the reduction of barite compacted samples (zone C; see Figure 1) with brown coal.

In the first 18 min at 900 and 950 °C and in the first 13 min at 1050 and 1150 °C, the values of the $BaSO_4$ to BaS conversion degree were close to those observed for zone A (the latter had only 5–7% higher values). However, later in the process the degree of conversion after 23 min reached a plateau for all studied temperatures: the maximum values were 0.25, 0.38, 0.47, and 0.51 at 900, 950, 1050, and 1150 °C, respectively. Such striking differences between the degree of conversion of barite located in the central (A) and extreme (C) zones can be explained as follows. According to conventional wisdom, the initial reduction of barite with carbon takes place via Equation (1). In this reaction, both barite and carbon are in contact with each other. This interaction prevails in the overall process of barite reduction, meaning that there is no significant difference in the degree of barite conversion in the central and outer zones in the first 13–18 min. In the case of the central zone, the formed carbon monoxide further reacts with barite to form carbon dioxide (Equation (2)), then the latter reacts with carbon according to the Boudouard reaction (Equation (3)) to form carbon monoxide. The carbon monoxide diffuses through the formed barium sulfide to the surface of the unreacted barium sulfate and reduces it according to Equation (2). In the case of the outer zone (zone C), the carbon monoxide formed according to Equation (1) predominantly leaves the reaction zone and diffuses into the atmosphere. Thus, the main source of barium sulfide is the initial reduction reaction of barium sulfate with solid carbon, while the gaseous intermediate (CO) is mostly lost. Unreacted barium sulfate is surrounded by a solid product (BaS), and remains almost unchanged. This explains the significant decrease in the degree of conversion of barite in the outer zone in comparison with the barite in the central zone of a compact cylindrical sample.

We now consider the conversion process of barite located in the intermediate zone (zone B). The dependence of the degree of barite conversion on the duration of heat treatment and temperature is shown in Figure 7.

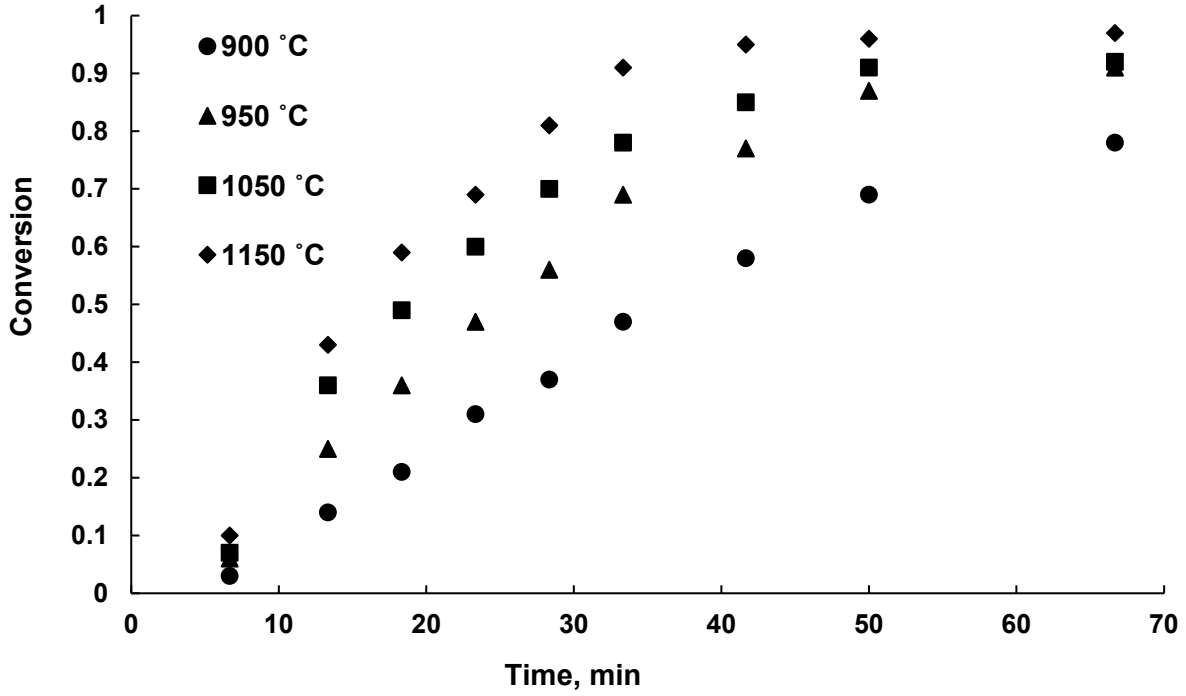

Figure 7. Conversion-time plots for the reduction of barite compacted samples (zone B; see Figure 1) with brown coal.

A comparison of the data presented in Figures 3 and 7 shows that the barite conversion of zones A and B was practically the same in the first 23 min for all temperatures studied. With a further increase in the duration of heating, for temperatures of 900 and 950 °C the conversion of barite in zone B was higher than that in zone A by 5–7% and 3–4%, respectively. For temperatures of 1050–1150 °C, the degree of barite conversion in zones A

and B was the same. The increase in barite conversion in the intermediate zone compared to the central zone can be explained as follows. Carbon monoxide produced according to Equations (1) and (3) moves from the central zone towards the atmosphere due to diffusion, passing through the intermediate and outer zones. Thus, the concentration of carbon monoxide in the intermediate zone is higher than in the central zone, which explains the higher degree of conversion in zone B compared to zone A.

With increasing temperature, this effect levels off, presumably due to the endothermicity of the solid-phase reduction reaction of barium sulfate with carbon (Equation (1)). Elevated temperatures (1050 and 1150 °C) lead to an increase in the concentration of CO in reaction zones A and B, and the diffusion of carbon dioxide described above no longer plays a decisive role in the reduction of barium sulfate.

The rate constants that describe the overall multi-stage process of barium sulfate conversion to barium sulfide for the whole compacted sample at all operating temperatures are presented in Table 1.

Table 1. Rate constants for the reduction of barite compacted sample (zone A) with brown coal.

Temperature, °C	900	950	1050	1150
Rate constant, $\times 10^5$ s^{-1}	2.03	2.59	4.20	5.82

Arrhenius plot for barium sulfate conversion created using the calculated rate constants (Figure 8).

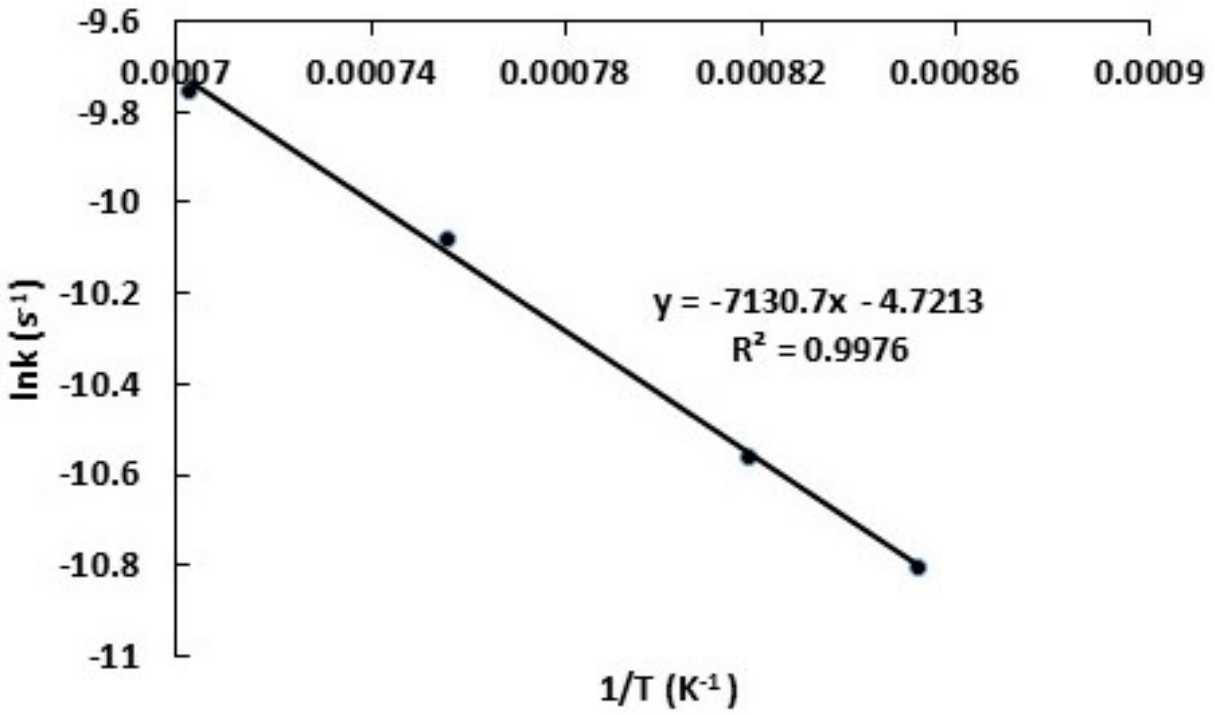

Figure 8. Arrhenius plot for barium sulfate conversion in the compacted sample.

The activation energy (E_a) of the overall chemical reaction determining $BaSO_4$ conversion into BaS was determined using Arrhenius's law (Equation (11)) [28]:

$$\ln k = -\frac{E_a}{R}\left(\frac{1}{T}\right) + \ln A \quad (11)$$

where k is the rate constant of the chemical reaction, R is the universal gas constant, and T is absolute temperature.

The calculated E_a was 136 kJ mol^{-1}. This value is much lower than those obtained earlier for the carbothermal reduction of barite. Jamshidi et al. achieved a value of about 293 kJ mol^{-1} for a powder batch and about 209 kJ mol^{-1} for an extruded charge [18]. Salem et al. obtained a value of about 200 kJ mol^{-1} during the carbothermal reduction of an extruded charge. The mechanical activation of the charge led to a decrease in the activation energy of the carbothermal reduction of barite from 519 to 276 kJ mol^{-1} [15]. At the same time, the use of sodium metavanadate as a catalyst made it possible to reduce the activation energy of barium sulfate conversion to 21 kJ mol^{-1} [16]. However, the economic feasibility of using sodium metavanadate in the carbothermal reduction of barite is questionable.

3.2. Powder Sample

The effect of operating temperature and treatment duration on the conversion of a powder barite sample to barium sulfide is shown in Figure 9.

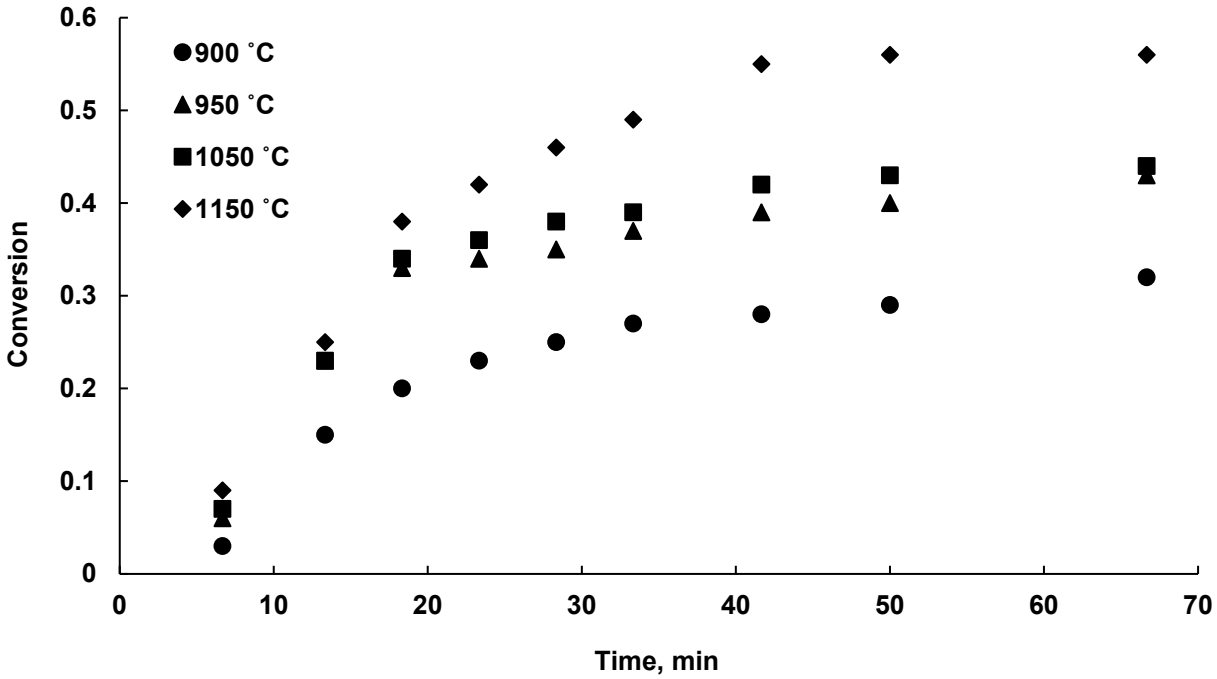

Figure 9. Conversion-time plots for the reduction of barite powder sample with brown coal.

As in the case of compact samples, an increase in the roasting duration, led to an increase in the degree of conversion of barium sulfate followed by the achievement of a plateau, as expected. The maximum degree of conversion was 0.6 when the charge was roasted at 1150 °C for 42 min. Such a low degree of conversion can be explained by the short duration of contact between carbon monoxide and barium sulfate due to the porosity of the charge; the rate of diffusion of carbon monoxide formed as a result of Reaction (2) is higher than in a compact sample.

The rate constants describing the process of barium sulfate conversion to barium sulfide at all operating temperatures in the case of the powder sample are presented in Table 2, and the Arrhenius plot for barium sulfate conversion in the powder sample is presented in Figure 10.

Table 2. Rate constants for the reduction of barite powder sample with brown coal.

Temperature, °C	900	950	1050	1150
Rate constant, $\times 10^5$ s^{-1}	0.48	1.24	2.56	4.19

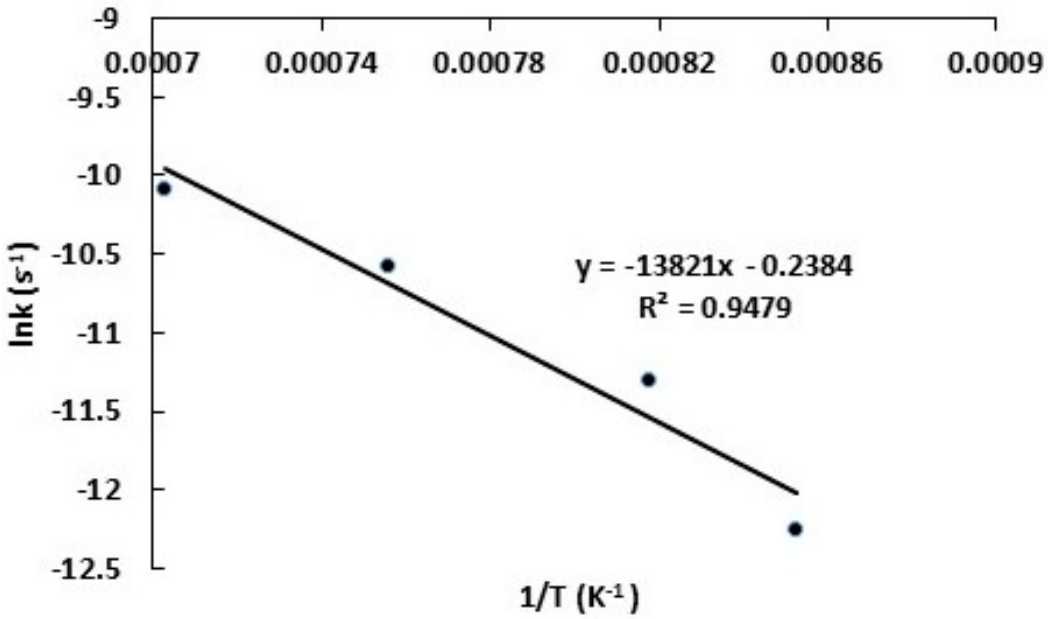

Figure 10. Arrhenius plot for barium sulfate conversion in powder sample.

A comparison of the data in Tables 1 and 2 shows a significant decrease in the barite conversion rate constants when moving from compact to powder samples, and this difference increases at lower temperatures: at 900 °C, the decrease was more than four times (2.03×10^{-5} vs. 0.48×10^{-5} s^{-1}), while at 1150 °C the difference was less than 30% (5.82×10^{-5} vs. 4.19×10^{-5} s^{-1}). The calculated activation energy in the case of the powder sample was 264 kJ mol^{-1}, which is almost twice that observed for the compact sample. Thus, charge compaction plays a beneficial role in reducing the activation energy of the barite carbothermal reduction, which can be used to reduce the energy intensity of the process.

4. Conclusions

In this article, we have shown that compaction of the charge before the carbothermal reduction of barite significantly enhances the conversion of barium sulfate to sulfide. This effect is associated with an increase in the contact time of carbon monoxide with barite in a compact sample in comparison with a powder sample; due to the lower porosity of a compact sample, the duration of diffusion of carbon monoxide from the charge into the atmosphere increases. In addition, the degree of reduction of barite in a compact sample differs depending on the environment of the charge; the maximum conversion of barite located at the sample–air interface did not exceed 0.51, while the conversion of barite closer to the central part of the sample (zone B) was 0.95–0.97. The charge compaction reduced the conversion activation energy (136 vs. 264 kJ mol^{-1}), which can be a tool for reducing the energy intensity of obtaining barium sulfide from its sulfate.

Author Contributions: Conceptualization, T.K. and R.N.; methodology, K.K. and A.B.; investigation, R.N., K.K. and A.B.; data curation, T.K.; writing—original draft preparation, R.N.; writing—review and editing, T.K. and R.N.; visualization, K.K. and A.B.; project administration, T.K. and R.N.; funding acquisition, T.K. All authors have read and agreed to the published version of the manuscript.

Funding: This research was funded by the Science Committee of the Ministry of Education and Science of the Republic of Kazakhstan (Grant No. OR11465430).

Data Availability Statement: The data supporting the results can be made available from the corresponding author upon request.

Conflicts of Interest: The authors declare no conflict of interest.

References

1. Ripin, A.; Mohamed, F.; Choo, T.F.; Yusof, M.R.; Hashim, S.; Ghoshal, D.S. X-ray shielding behaviour of kaolin derived mullite-barites ceramic. *Radiat. Phys. Chem.* **2018**, *144*, 63–68. [CrossRef]
2. Da Silva, M.J.; Bartolome, J.F.; Antonio, H.; Mello-Castanho, S. Glass ceramic sealants belonging to BAS ($BaO–Al_2O_3–SiO_2$) ternary system modified with B_2O_3 addition: A different approach to access the SOFC seal issue. *J. Eur. Ceram. Soc.* **2016**, *36*, 631–644. [CrossRef]
3. Zhang, W.; Zhang, F.; Ma, L.; Yang, J.; Yang, J.; Xiang, H. Reaction mechanism study of new scheme using elemental sulfur for conversion of barite to barium sulfide. *Powder Technol.* **2020**, *360*, 1348–1354. [CrossRef]
4. Diós, P.; Szigeti, K.; Budán, F.; Pócsik, M.; Veres, D.S.; Máthé, D.; Nagy, S. Influence of barium sulfate X-ray imaging contrast material on properties of floating drug delivery tablets. *Eur. J. Pharm. Sci.* **2016**, *95*, 46–53. [CrossRef] [PubMed]
5. Guzmán, D.; Fernández, J.; Ordoñez, S.; Aguilar, C.; Rojas, P.A.; Serafini, D. Effect of mechanical activation on the barite carbothermic reduction. *Int. J. Miner. Process.* **2012**, *102*, 124–129. [CrossRef]
6. Vakilpour, S.; Ghaderi Hamidi, A. Effects of Temperature and Particle Size Distribution on Barite Reduction by Carbon monoxide Gas. *J. Part. Sci. Technol.* **2016**, *2*, 79–85.
7. Mulopo, J.; Motaung, S. Carbothermal reduction of barium sulfate-rich sludge from acid mine drainage treatment. *Mine Water Environ.* **2014**, *33*, 48–53. [CrossRef]
8. Ravdel, A.; Novikova, N. Reduction of barite with carbon. *J. Appl. Chem.* **1963**, *36*, 1384–1392.
9. Pelovski, Y.; Gruchavov, I.; Dombalov, I. Barium sulfate reduction by carbon in presence of additives. *J. Therm. Anal.* **1987**, *32*, 1743–1745. [CrossRef]
10. McKee, D.W. Mechanisms of the alkali metal catalysed gasification of carbon. *Fuel* **1983**, *62*, 170–175. [CrossRef]
11. Lozhkin, A.F.; Pashcenko, V.N.; Povar, F.V. Kinetics of Reduction of Barite by Roasting with Carbon. *J. Appl. Chem.* **1974**, *47*, 1031–1034.
12. Jagtap, S.B.; Pande, A.R.; Gokarn, A.N. Effect of catalysts on the kinetics of reduction of barite by carbon. *Ind. Eng. Chem. Res.* **1990**, *29*, 795–799. [CrossRef]
13. McKee, D.W.; Chatterji, D. The catalytic behavior of alkali metal carbonates and oxides in graphite oxidation reactions. *Carbon* **1975**, *13*, 381–390. [CrossRef]
14. Kumar, J. Effect of Sodium Compounds on Reduction of Barite at High Temperature: A Comparative Study. *Mater. Today Proc.* **2019**, *16*, 870–874. [CrossRef]
15. Salem, A.; Tavakoli, O.Y.; Jamshidi, S. Kinetic study of barite carbothermic reduction in presence of sodium carbonate as catalyst. *Iran. J. Chem. Eng.* **2010**, *7*, 58–67.
16. Gokarn, A.N.; Pradhan, S.D.; Pathak, G.; Kulkarni, S.S. Vanadium-catalysed gasification of carbon and its application in the carbothermic reduction of barite. *Fuel* **2000**, *79*, 821–827. [CrossRef]
17. Agrawal, R.K. The compensation effect: A fact or a fiction. *J. Therm. Anal.* **1989**, *35*, 909–917. [CrossRef]
18. Jamshidi, S.; Salem, A. Role of extrusion process on kinetic of carbothermal reduction of barite. *Thermochim. Acta* **2010**, *503*, 108–114. [CrossRef]
19. Xiong, N.; Tian, Y.; Yang, B.; Xu, B.Q.; Dai, T.; Dai, Y.N. Results of recent investigations of magnesia carbothermal reduction in vacuum. *Vacuum* **2019**, *160*, 213–225. [CrossRef]
20. Li, K.; Chen, J.; Peng, J.; Ruan, R.; Srinivasakannan, C.; Chen, G. Pilot-scale study on enhanced carbothermal reduction of low-grade pyrolusite using microwave heating. *Powder Technol.* **2020**, *360*, 846–854. [CrossRef]
21. Zhang, H.; Ruan, Y.; Liang, A.; Shih, K.; Diao, Z.; Su, M.; Hou, L.; Chen, D.; Lu, H.; Kong, L. Carbothermal reduction for preparing nZVI/BC to extract uranium: Insight into the iron species dependent uranium adsorption behavior. *J. Clean. Prod.* **2019**, *239*, 117873. [CrossRef]
22. Agrawal, S.; Rayapudi, V.; Dhawan, N. Comparison of microwave and conventional carbothermal reduction of red mud for recovery of iron values. *Miner. Eng.* **2019**, *132*, 202–210. [CrossRef]
23. Yang, S.; Ma, W.; Wei, K.; Xie, K.; Wang, Z. Thermodynamic analysis and experimental verification for silicon recovery from the diamond wire saw silicon powder by vacuum carbothermal reduction. *Sep. Purif. Technol.* **2019**, *228*, 115754. [CrossRef]
24. Yeşiltepe, S.; Buğdaycı, M.; Yücel, O.; Şeşen, M.K. Recycling of alkaline batteries via a carbothermal reduction process. *Batteries* **2019**, *5*, 35. [CrossRef]
25. Snell, F.D.; Hilton, L. *Encyclopedia of Industrial Chemical Analysis*; Wiley: Hoboken, NJ, USA, 1984.
26. Kasaoka, S.; Sakata, Y.; Kayano, S.; Masuoka, Y. The Development of Rate Expressions and the Evaluation of Reactivity for Gasification of Various Coal Chars with Steam and Oxygen. *Int. Chem. Eng.* **1983**, *23*, 477–485.
27. Kasaoka, S.; Sakata, Y.; Tong, C. Kinetic Evaluation of the Reactivity of Various Coals Chars for Gasification with Carbon Dioxide in Comparison with Steam. *Int. Chem. Eng.* **1985**, *25*, 161–175. [CrossRef]
28. Levenspiel, O. *Chemical Reaction Engineering*; John Wiley & Sons: Hoboken, NJ, USA, 1999; p. 684.